Heliyon 10 (2024) e37110

Contents lists available at ScienceDirect

Heliyon

journal homepage: www.cell.com/heliyon

Research article

Anti-vasodilator-stimulated phosphoprotein (VASP) antibodies are associated with neuropsychiatric disorders in systemic lupus erythematosus

Chenxi Zhu [a], Yan Liu [b], Jiayi Xu [b], Hang Yang [b], Yi Zhao [a,b,*], Yi Liu [b]

[a] Department of Rheumatology and Immunology, Clinical Institute of Inflammation and Immunology, Frontiers Science Center for Disease-related Molecular Network, West China Hospital, Sichuan University, Chengdu, Sichuan, China
[b] Department of Rheumatology and Immunology, West China Hospital, Sichuan University, Chengdu, Sichuan, China

ARTICLE INFO

Keywords:
Neuropsychiatric involvement
Vasodilator-stimulated phosphoprotein
Neo-antigen
Autoimmunity

ABSTRACT

Background: Systemic lupus erythematosus (SLE) is a complex autoimmune disease characterized by multi-organ involvement and the presence of autoantibodies, pathogenic factors that can serve as diagnostic biomarkers. The current research has been focusing on exploring specific autoantigens with clinical relevance for SLE subtypes. In line with this objective, this study investigated potential antigenic targets associated with specific phenotypes in SLE by leveraging an omics-based approach combined with immunoassay techniques.

Methods: A transcriptomic analysis was conducted in a cohort of 70 SLE patients to identify genes significantly correlated to the relevant phenotype. Epitope mapping and sequence analysis techniques were used to predict autoantigens, and the corresponding antibodies were subsequently quantified by enzyme-linked immunosorbent assay (ELISA) and validated by Western blot.

Results: Transcriptomic data analysis revealed a group of hub genes exhibiting a significant correlation with the neuropsychiatric phenotype and a positive relationship with platelets. Subsequent epitope prediction for the corresponding proteins highlighted vasodilator-stimulated phosphoprotein (VASP) as a potential autoantigen. Moreover, ELISA and immunoblotting confirmed that the anti-VASP antibody present in the serum was significantly elevated in SLE patients with neuropsychiatric involvement and positively associated with demyelination.

Conclusion: VASP harbors autoantigenic epitopes associated with neuropsychiatric phenotype, especially the demyelination symptom in SLE, and its antibodies may serve as promising biomarkers in this disease.

1. Background

Systemic lupus erythematosus (SLE) is a complex autoimmune disease that can affect multiple organs in the body, resulting in various symptoms ranging from mild to severe [1]. There is broad agreement that the accumulation of autoantibodies in the

* Corresponding author. Department of Rheumatology and Immunology, Clinical Institute of Inflammation and Immunology, Frontiers Science Center for Disease-related Molecular Network, West China Hospital, Sichuan University, Department of Rheumatology and Immunology, West China Hospital, Sichuan University, Chengdu, Sichuan, China.
E-mail addresses: chenxizhu1995@gmail.com (C. Zhu), zhaoyi-rheuma@wchscu.cn (Y. Zhao), yiliu_2020@scu.edu.cn (Y. Liu).

https://doi.org/10.1016/j.heliyon.2024.e37110
Received 19 March 2024; Received in revised form 22 August 2024; Accepted 27 August 2024
Available online 31 August 2024

bloodstream has a crucial role in developing SLE [2]. The autoantibodies are produced by autoreactive B cells, which become activated through helper T cells [3]. The autoantibodies can recognize or cross-react with self-components, typically ribonucleoprotein and double-stranded DNA [4], resulting in the formation and deposition of immune complexes [5]. They can also cause tissue damage in SLE [5]. The SLE risk factors, like viral and bacterial infections, may cause epitope spreading through antigenic drive within autoreactive germinal centers, promoting clonal evolution and autoantibody diversification [6]. Under persistent inflammation, damaged host cells release autoantigenic nuclear components despite neutrophil extracellular traps, a commonly known source of DNA [7]. Moreover, a previous study found that platelets can release mitochondrial DNA after the stimulation of platelet FcγRIIA [8].

Recent studies in the field have been focusing on identifying autoantigens that may participate in the development of SLE. However, given the heterogeneity of SLE, the diagnostic efficacy of different autoantibodies varies among different subtypes of patients [9]. Despite extensive research into the biomarkers of SLE, the effective indicators of different phenotypes of the disease remain limited [10]. Thus, it is of utmost importance to investigate the clinical relevance of autoantigens to develop precise diagnoses and targeted therapies for different subsets of patients.

Advances in genomic and proteomic biology have enabled researchers to classify patients better based on molecular and clinical features [11]. This study identified a novel autoantibody targeting the VASP as a potential biomarker for neuropsychiatric involvement in SLE. Initially, we conducted a transcriptomic analysis of 70 SLE patients and used clustering gene expression data to divide samples into two clusters, one of which had a significantly larger proportion of patients with neuropsychiatric syndrome. Subsequently, weighted gene co-expression network analysis (WGCNA) was used to identify a gene module highly correlated with this cluster. Further analysis revealed that these genes are related to nervous inflammation and platelet activation. We then utilized epitope mapping to identify one gene, VASP, whose corresponding protein was expressed in blood platelets and brain tissue, as a potential autoantigen. Our data were subsequently confirmed through ELISA, demonstrating a positive correlation between anti-VASP antibodies and neuropsychiatric involvement, especially the demyelination symptom, implicating VASP as a potential diagnostic biomarker for this SLE phenotype.

2. Methods

2.1. Study subjects

A total of 70 SLE patients were recruited through the rheumatology outpatient clinic, and 19 healthy controls (HCs) matched for age and gender were recruited during the physical examination in West China Hospital. Patients diagnosed with SLE based on the American College of Rheumatology criteria from 2019 [12] whose condition was reassessed at our outpatient clinic within the past three months and who underwent blood tests, imaging studies, or pathological examinations at our hospital, were enrolled. SLE patients were then classified into two subgroups: (1) those without neuropsychiatric involvement (other SLE group) and (2) those with neuropsychiatric involvement (NPSLE group). Patients with NPSLE met the ACR 1999 criteria for NPSLE [13]. Demyelination in NPSLE was diagnosed based on magnetic resonance imaging (MRI) findings; all patients with demyelinating NPSLE met the 1999 ACR criteria for demyelination [13]. HCs included individuals visiting the clinic for reasons unrelated to autoimmunity or surgery unrelated to inflammatory diseases and were matched for age and gender. Only individuals who voluntarily joined the study after being informed of the research content by the researchers were included.

Peripheral blood and serum were collected from all subjects. All patients' clinical information, including disease activity index (SLEDAI2000), involvement of organs, and clinical tests such as MRI, blood/urine routine, inflammatory factors, anti-dsDNA antibody, and ANA (chemiluminescence method) were collected through outpatient services.

Ethical approval was obtained from the Committee for Ethics of West China Hospital, Sichuan University, China. Also, all patients signed the informed consent form.

2.2. RNA sequencing

Whole RNA was isolated from blood, subjected to qualification, and quantified by NanoDrop 2000 and Agilent 2100/4200 system. mRNA was extracted from the total RNA to construct the library. After pooling different samples, they were subjected to Illumina sequencing (paired-end 150). Raw data written in the FASTQ file were refined by quality control. After removing rRNA, clean reads were aligned to the reference genome using Hisat2. Finally, read counts were obtained by mapping using Featurecount.

2.3. Weighted gene Co-expression network analysis

First, we calculated the Median Absolute Deviation for each gene and identified the top 50 % of genes with significant variation, which we referred to as GoodSamplesGenes. Next, GoodSamplesGenes was used to construct a scale-free co-expression network, removing outlier genes. Pearson's correlation matrices and average linkage method were used for all genes relative to one another. A soft-thresholding parameter of 8 (Fig. 2A) was chosen as it allowed us to transform the adjacency into a topological overlap matrix (TOM), which was next used to perform the average linkage hierarchical clustering, based on a TOM-based dissimilarity measure to identify gene modules with similar expression profiles. The minimum size of the genes dendrogram was set at 30, with a sensitivity of 3. After calculating the dissimilarity of all modules, we selected a cut line for the dendrogram and merged those modules within 0.25 distance. Ultimately, 21 co-expression modules (Fig. 2B and C) were obtained; all analyses were conducted using the WGCNA R package [14].

2.4. Statistical analysis

Normalization and differential analysis of the RNA expression matrix were performed using the DESeq2 R package (please cite the reference). The thresholds for differentially expressed genes were set at FDR <0.05 and fold change >2 [15]. GO annotation, KEGG, reactome and Wikipathway enrichment of the selected gene module was implemented using "ClusterProfiler" package [16]. Adj. p value <0.05 was considered statistically significant. Protein-Protein Interaction Network Construction (PPI) network was retrieved using the STRING database based on the corresponding protein names in the target module [17]. Those connected ones were extracted from the whole net. A confidence score of ≥ 700 was set as the parameter for significance. A network diagram was constructed on the original page.

2.5. Epitope prediction

For homologous alignment, we applied the epitope conservancy analysis tool [18](at http://tools.immuneepitope.org/tools/conservancy) to determine the variability of SLE epitopes within protein sequences of candidate hub genes. The identity threshold was set at $>$ 75 %. After screening out the optimal sequences, they were subjected to biophysical properties analysis and secondary structure prediction via Protean software. Garnier-Robson/Chou-Fasman predicted the alpha, beta, turn, and coil regions. The amphipathic regions, hydrophilicity, flexibility, and antigenicity were analyzed using Eisenberg, Karplus-Schulz, and Jameson-Wolf algorithm.

2.6. ELISA

Anti-VASP and ANXA11 antibodies in serum were assessed using purified recombinant human VASP and ANXA11 purchased from Abcam company (Item No. ab105601 and No. ab101050). Firstly, 0.2 μg/well of proteins for coated wells or phosphate-buffered saline (PBS) for blank wells were added onto the 96-well plate with bicarbonate buffer (100 μL total volume/well, pH = 9.6) and coated overnight at 4 °C on the shaker. Then, 5 % Bovine Serum Albumin (BSA) in PBS was used to block, after which the wells were washed three times with PBST composed of 0.05 % Tween 20 in PBS. The wells were then incubated with diluted serums (1:100) for 90 min at 37 °C. Rabbit monoclonal antibodies targeting VASP and ANXA11 were purchased from Abcam company (Item No. ab109321 and No. ab236599) and used as the positive control (dilution was 1:20,000), while PBS was used as the negative control. After washing the wells five times with PBST, horseradish peroxidase (HRP)-linked anti-human/rabbit IgG Ab (dilution was 1:100000) was mixed and rested for 60 min at 37 °C. After a 15-min incubation with SureBlue 3,3′,5,5′-Tetramethylbenzidine microwell peroxidase substrate, the optical density (OD value) at 450 nm was detected by BioTek Synergy H1 Multimode Reader. All samples were normalized to a standard scale between 0 and 100, with the positive control defined as 100 and the lowest sample defined as 0. After adjusting the OD value by blank wells minus coated wells, different groups were compared using one-way ANOVA. Statistical analysis was conducted using GraphPad Prism 9.0.

2.7. Detection of anti-U1-snRNP and anti-SM antibodies

Antibodies against U1-snRNP and Sm were detected using the EUROLINE method with the Anti-ENA ProfilePlus 1 reagent (EUROIMMUN CN). The membrane strips were placed numbered side up in incubation troughs. After adding 1.5 mL of sample buffer and incubating at room temperature for 5 min, the buffer was discarded and replaced with 1.5 mL of diluted serum sample (1:100), which was incubated for 30 min. The serum was discarded, and the strips were washed three times with 1.5 mL of wash buffer. Consequently, 1.5 mL of diluted enzyme conjugate (alkaline phosphatase-labeled anti-human IgG) was added, and samples were incubated for 30 min. The conjugate was then discarded, and the strips were washed thrice with wash buffer. Then, 1.5 mL of substrate solution was added, and samples were incubated for 10 min. After discarding the substrate, the strips were washed three times with distilled water and air-dried on the result interpretation template. Scanning was performed with EUROIMMUN AG; EUROLineScan software was used for evaluation. Antibody levels were classified as 0, 1, 2, and 3, corresponding to negative, weak positive, positive, and strong positive, respectively.

2.8. Immunoprecipitation and immunoblotting

First, 50 μL of serum and 0.5ug VASP were incubated with 200 μL of IP buffer (PBS with 0.1 % (w/v) BSA +0.1 % (v/v) Tween 20) overnight at 4C. Then 40 μL of 50 % protein G sepharose was added to the mixture and incubated on the shaker for 2 h at 4 °C. After centrifugating at 2500 rpm for 5min, precipitations were collected and washed with IP buffer 3–5 times. Then, the samples were boiled for 5 min in sodium dodecyl sulfate buffer. After centrifugating, supernatants were subjected to electrophoresis on 12 % gel and transferred onto polyvinylidene fluoride membranes, blocked with 5 % (w/v) skim milk in PBS, and incubated with rabbit monoclonal to VASP (diluted to 1:1000) overnight at 4 °C. The VASP on the membrane was detected by HRP-conjugated anti-human/rabbit IgG antibody. Image analysis was performed on ChemiDoc™ MP Imaging System (Bio-Rad).

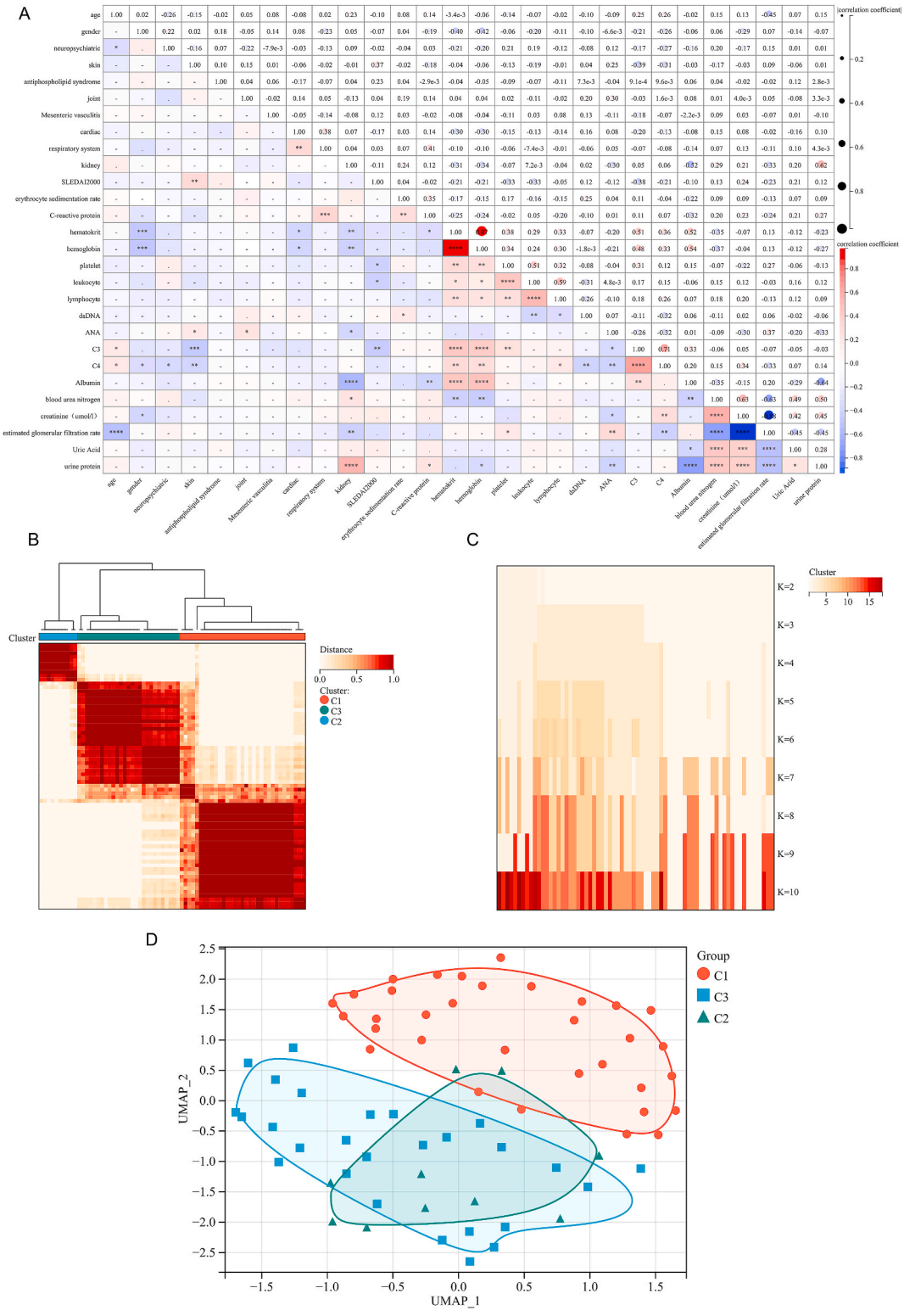

Fig. 1. **(A)** Spearman correlation test of clinical characteristics. Categorical variables like gender and organ involvements were redefined as follows: Male-1, Female-2; not involved-1, involved-2. **(B)** Consensus clustering using agglomerative kmdist clustering with a euclidean distance and 70 samples divided into 3 clusters (C1, C2, C3). **(C)** Trackingplotconsensus provides a view of item cluster membership across different k (2-10). **(D)** A dimensionality reduction projection (UMAP algorithm) of RNA-seq data verified that C1 and C2/3 have transcriptome differences.

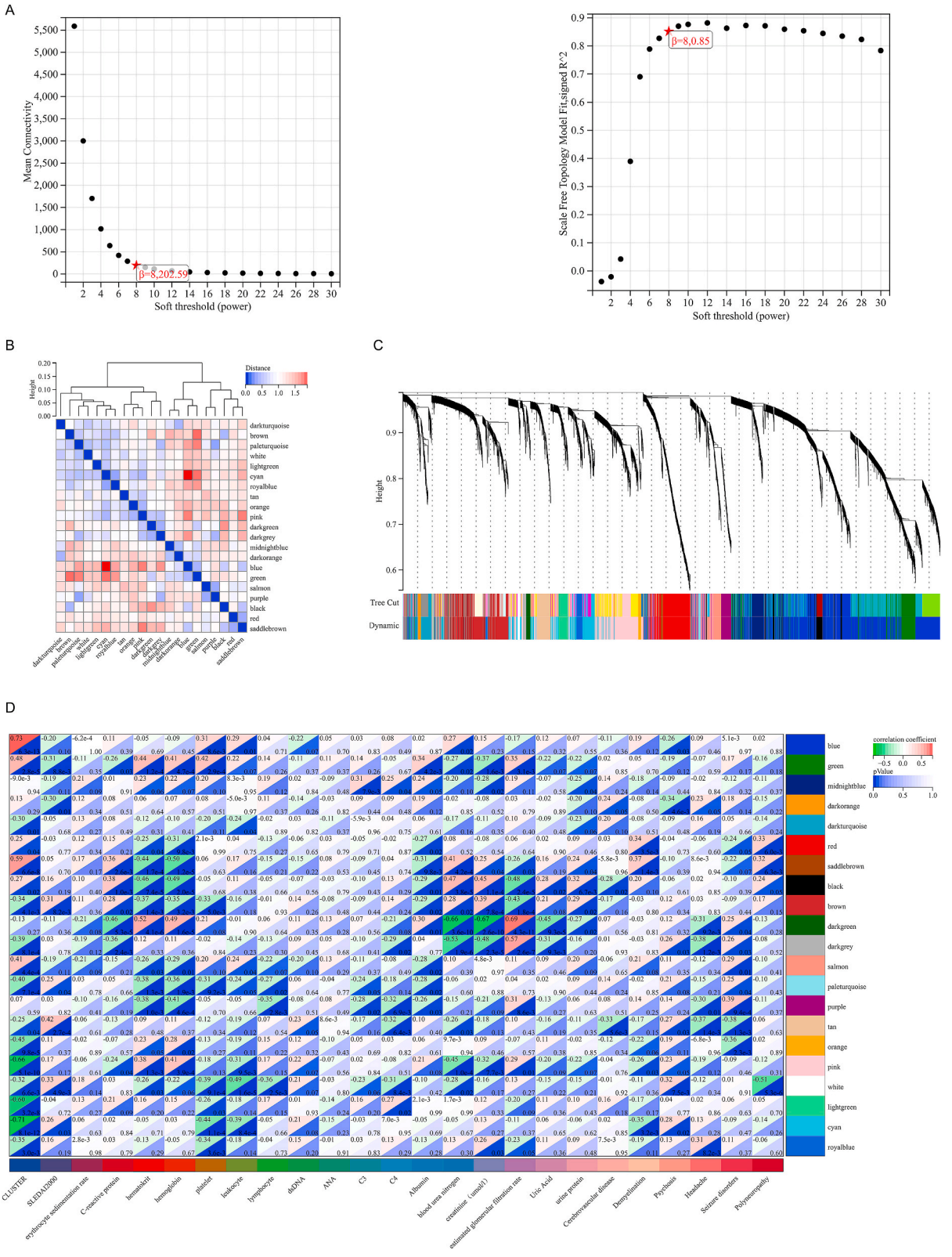

Fig. 2. **(A)** The soft threshold was determined by scale independence and mean connectivity. **(B)** Clustering of module eigengenes based on their similarity **(C)** Cluster dendrogram of merged modules. **(D)** Coefficients of co-expression modules with clinical characteristics.

3. Results

3.1. Identification of clusters linked to neuropsychiatric manifestation

A total of 70 patients, 61 females and 9 males aged between 25 and 50 years old and diagnosed with SLE between June 2020 and June 2021 at West China Hospital were recruited in this study. Medical history, data associated with clinical symptoms, laboratory examinations, and disease activity scores were collected for all patients. As shown by the results of multivariate correlation (Fig. 1A), in terms of organ involvement, patients with neuropsychiatric involvement were younger, primarily female, and had higher blood urea nitrogen (BUN) and platelet levels as well as lower C4 levels. Patients with skin involvement had a significant increase in SLEDAI score and decreased levels of C3 and C4. Patients with cardiovascular and renal involvement had lower red blood cell counts and hemoglobin levels, while the latter also had lower albumin levels, lower glomerular filtration rates, and significantly elevated BUN and urine protein levels. The correlation between organ involvement and laboratory examinations confirmed the reliability of our clinical data.

RNA sequencing and associated analyses were performed on the peripheral blood; the ConsensusClusterPlus algorithm was used to classify patients into three distinct clusters: C1, C2, and C3 (Fig. 1B and **C**). Further analysis, based on dimensionality reduction projection, confirmed that the transcriptomics pattern between C1 and the other two clusters was markedly different (Fig. 1D), resulting in the combination of C2 and C3 for subsequent analyses. Patients in C2 and C3 showed a significantly higher prevalence of neuropsychiatric involvement (abbreviated as NPSLE) with p value < 0.01, and there were no differences in other characteristics (Table 1). Overall, our transcriptome analysis revealed the presence of three distinct clusters of individuals. Two of these clusters exhibited genetic differences with the third one and had a greater prevalence of neuropsychiatric symptoms.

3.2. Identification of eigengene linked with neuropsychic involvement

Given the identified clusters connected with NPSLE, we sought to investigate the hub genes involved in the underlying pathogenesis by constructing a weighted gene co-expression network using the WGCNA R package. Our analysis yielded a total of 21 co-expression modules, among which the blue module showed the strongest correlation with the C2/3 ($R = 0.73$), while the saddle brown module was the second most correlated ($R = 0.59$), with a relatively small distance from the blue module (Fig. 2B and D). These modules were positively associated with platelet and leukocyte counts and BUN, which was consistent with the blood indicators that were elevated in NPSLE.

To further elucidate the relationship between the identified modules and specific clinical features, we conducted a comprehensive examination of the clinical characteristics of NPSLE patients, including MRI, electroencephalogram, and electromyography. As shown in Table 2, among all 28 NPSLE patients, there were 20 patients diagnosed with cerebrovascular disease, 15 patients with demyelination, 9 patients with psychiatric disorders, 9 patients with headaches, 3 patients with a history of epilepsy, and 6 patients with polyneuropathy. Correlation analysis indicated that neurological rather than psychiatric disorders were a primary clinical manifestation associated with genetic factors in NPSLE subsets. Specifically, we observed a positive correlation between the saddle brown

Table 1
Summary of organ involvement of SLE grouped by clusters.

Organ Involvements	C1 (N = 33)	C2/3 (N = 37)	*P* Value
Neuropsychiatric involvement			**0.0053**
No	26 (37.14 %)	16 (22.86 %)	
Yes	7 (10.00 %)	21 (30.00 %)	
Skin Involvement			0.39
No	19 (27.14 %)	26 (37.14 %)	
Yes	14 (20.00 %)	11 (15.71 %)	
Antiphospholipid Syndrome			0.82
No	26 (37.14 %)	31 (44.29 %)	
Yes	7 (10.00 %)	6 (8.57 %)	
Joint Involvement			0.77
No	23 (32.86 %)	28 (40.00 %)	
Yes	10 (14.29 %)	9 (12.86 %)	
Mesenteric Vasculitis			0.84
No	30 (42.86 %)	32 (45.71 %)	
Yes	3 (4.29 %)	5 (7.14 %)	
Cardiac Involvement			0.65
No	24 (34.29 %)	24 (34.29 %)	
Yes	9 (12.86 %)	13 (18.57 %)	
Respiratory System Involvement			0.845
No	28 (40.00 %)	32 (45.71 %)	
Yes	5 (7.14%)	5 (7.14 %)	
Kidney Involvement			0.77
No	10 (14.29 %)	9 (12.86 %)	
Yes	23 (32.86 %)	28 (40.00 %)	

Variables were presented as percentages, and Chi-squared tests were performed to compare differences with statistical significance indicated by bold values: $p < 0.05$.

Table 2
The summary of neuropsychiatric symptoms in 28 NPSLE.

Neuropsychiatric syndromes	with	without
Cerebrovascular disease	20(71.43 %)	8(28.57 %)
Demyelination	15(53.57 %)	13(46.43 %)
Psychosis	9(32.14 %)	19(67.86 %)
Headache	9(32.14 %)	19(67.86 %)
Seizure disorders	3(10.71 %)	25(89.29 %)
Polyneuropathy	6(21.43 %)	22(78.57 %)

module and polyneuropathy ($p = 0.0063$) and demyelination ($p = 0.0014$), while psychosis incidents were negatively related to the blue module ($p = 0.03$).

We then conducted a co-expression network construction and association analysis with clinical features, identifying two modules showing strong correlations with nerve damage in SLE. These modules provided potential gene targets interpreting the relationship between transcriptome and clinical phenotype.

3.3. Hub genes are involved in immune and neuroinflammation-related pathways

We comprehensively analyzed essential genes and their functions to investigate potential pathogenic mechanisms involving genes associated with neural injury. By examining the expression of individual genes in relation to specific clusters, gene significance (GS) values were calculated. In addition, the correlation between the expression of module feature vectors and genes was calculated to determine module membership (MM) values. A total of 543 and 30 highly interconnected genes strongly associated with the C2/3 subset in the blue and saddle brown modules, respectively, were identified using a cut-off criterion ($|MM| > 0.8$ and $|GS| > 0.1$). As depicted in Fig. 3A, the MM and GS values of the hub genes were significantly correlated, indicating that these genes have a critical role in the module and are strongly linked to the clinical trait.

Further analysis revealed that these genes were primarily involved in the biological processes of neutrophil degranulation, protein phosphorylation, and inflammatory response. Interestingly, these genes were not located explicitly in cellular components, but rather, their functions were enriched in protein binding and certain kinase activities (Fig. 3B). Wikipathway enrichment analysis showed that several inflammation pathways, such as interleukin (IL)-4, IL-6, Th17 cell differentiation, and B cell receptor signaling pathways, were significantly enriched. Moreover, we found that the hub genes were significantly activated in neuroinflammation and glutamatergic signaling (Fig. 3C). KEGG analysis indicated that these genes are involved in innate and adaptive immunity pathways. Additionally, we observed that the neurotrophic signaling pathway may contribute to the association of the module with NPSLE (Fig. 3D).

Based on the function enrichment analysis, it can be inferred that the hub genes were associated with immunity and potentially significantly impacted the development of neural injury.

Next, differential analyses were performed between 28 NPSLE and 42 other SLE subgroups. Screening criteria for differential genes (DEG) were: 2-fold change, FDR<0.05. In the NPSLE, 233 DEGs were up-regulated, while 28 DEGs were down-regulated (Fig. S1A). The enrichment analysis indicated that upregulated DEGs were associated with the ankyrin-1 complex and erythrocyte-related functions, such as carbon dioxide transport and porphyrin metabolism (Figs. S1B and S1C). The top items of downregulated DEG were primarily related to complement activation, a key component of innate immunity. This data suggested that NPSLE patients may exhibit less inflammation compared to other SLE group. Additionally, synapse pruning, a crucial process in nervous system development, was significantly enriched (Figs. S1D and S1E). According to previous reports, alteration in the synapse pruning process has been associated with a variety of neurodevelopmental disorders and mental diseases [19].

3.4. Computational prediction of autoantigens related to neuroinflammation by epitope conservancy and antigenicity analysis

As indicated previously, there is a potential relationship between the upregulation of hub genes and inflammation in the nervous system. One key mechanism of neuronal injury is the immune response to autoantigens. In autoimmune conditions, autoantigens can activate autoreactive T cells, mainly T follicular helper (TFH) cells, stimulating B cells to produce antibodies. T-cell activation depends on the antigen dose, with TFH cell response influenced by antigen levels [20,21]. Thus, we hypothesized that genes with elevated transcription in the NPSLE group, especially those with antigenic epitopes, are likely to serve as potential antigens due to their increased abundance. To identify pathogenic targets, we analyzed the corresponding proteins of the genes in terms of antigenicity.

We retrieved immunogenic antigens associated with autoimmune diseases of the nervous system from the Immune Epitope Database (IEDB) [22]. After removing duplicates and mapping to gene symbols, 621 antigens overlapping with hub genes were identified. Using a Venn diagram (Fig. 4A), 26 candidates were selected for further antigenic analysis; corresponding protein sequences for these 26 candidates were obtained from Uniprot [23].

The following search strategy was applied to the IEDB: ‘peptide’, ‘SLE’, ‘T cell assay’, ‘B cell assay’, and ‘MHC ligand’ to identify all possible epitopes. Small fragments were excluded by setting the optimal length >8 amino acids (aa), which resulted in 899 epitopes with lengths between 8 and 50aa.

Using the Epitope Conservancy Analysis tools, we conducted homologous alignment and calculated the degree of conservancy of 899 epitopes within protein sequences corresponding to the 26 genes. As shown in Table 3, 25 SLE peptides derived from small nuclear

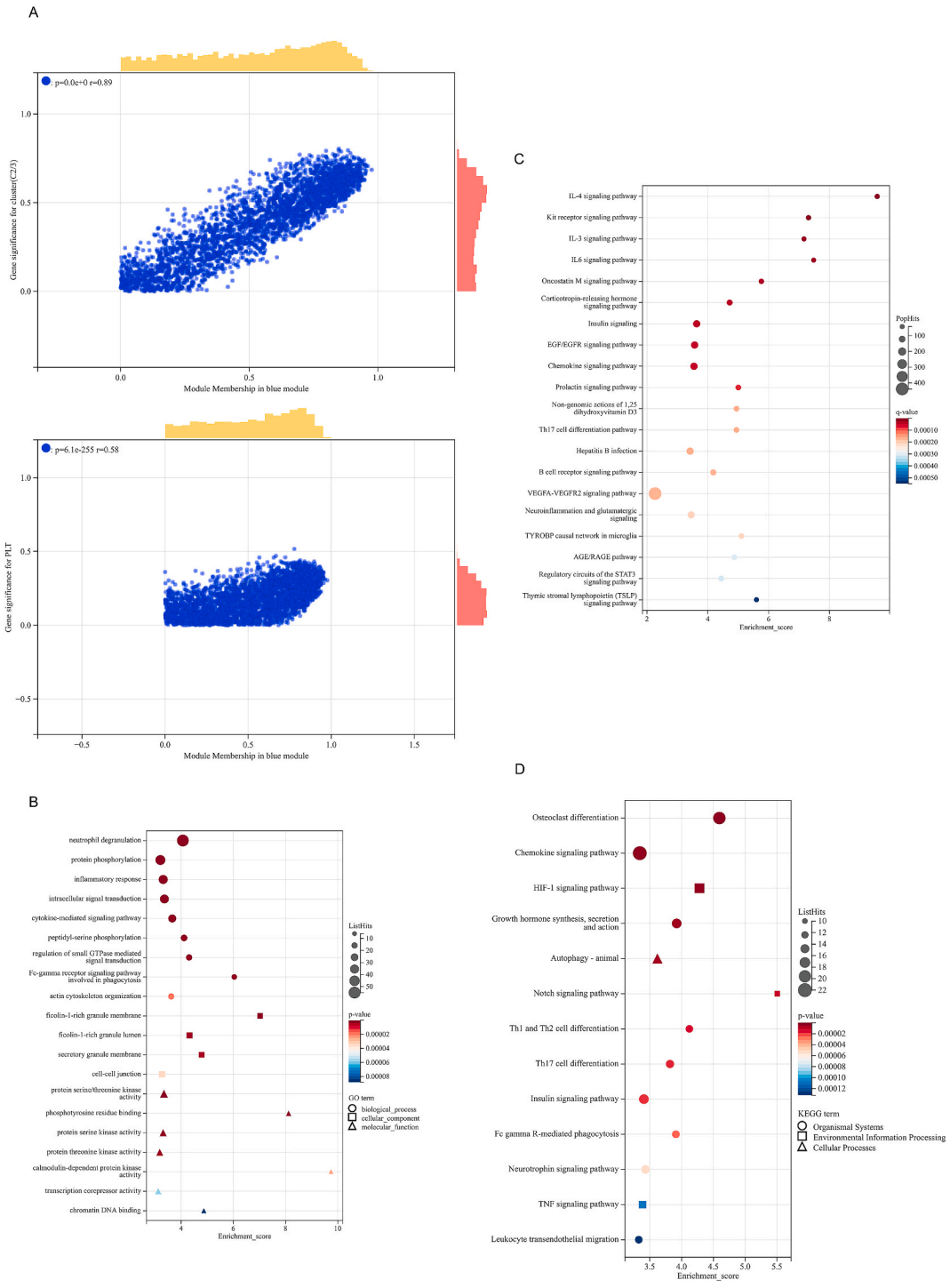

Fig. 3. **(A)** Correlation of gene significance for the cluster with module membership in the blue and saddle brown module. **(B–D)** GO (B), Wiki-pathway (C), and KEGG (D) enrichment of the hub genes.

ribonucleoprotein polypeptide B, U1 small nuclear ribonucleoprotein A (U1-snRNP), and U1 small nuclear ribonucleoprotein C had identities over 75 % with certain candidate sequences. Specifically, we identified six proteins with homology with SLE epitopes, with VASP, CBP (gene name: CREBBP), and ANX11 having the most detected sequences.

After concatenating sequences head-to-tail to join longer ones, we further predicted the antigenicity of these sequences in proteins using the DNAStar Protean program (Table 4, Table S1, and Table S2). Our results showed that VASP had an acceptable hydrophilicity

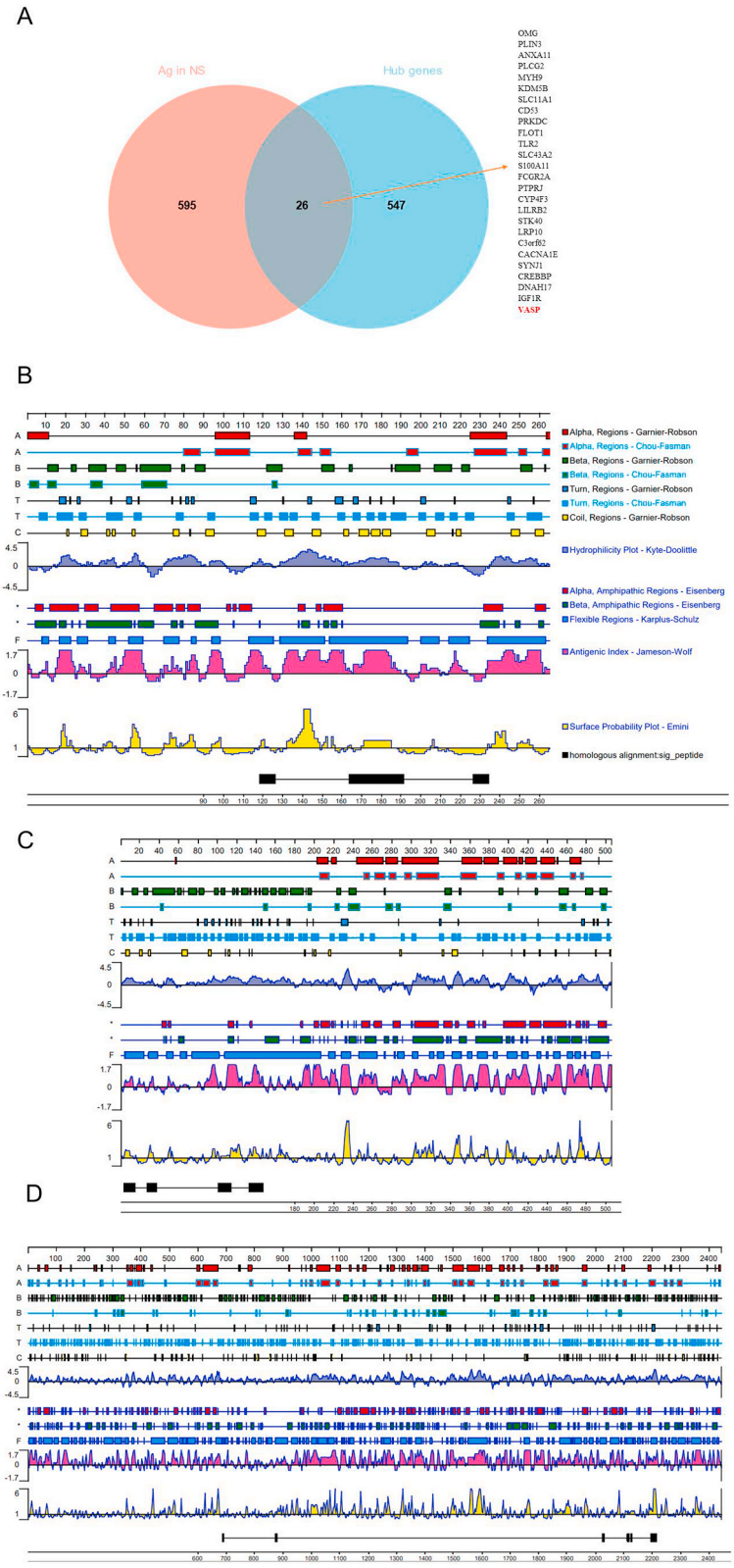

Fig. 4. **(A)** Venn diagram showing overlap of Ag for autoimmune diseases of the nervous system and hub genes in blue and saddle brown modules. **(B–D)** Secondary structure prediction, hydrophilicity, antigenic index, and surface probability with aligned fragments plots of VASP (B), ANX11 (C), and CBP (D).

Table 3
The representative results for homologous alignment.

Epitope sequence	Antigen Name	Protein name	Positions	Protein sub-sequence(s)	Identity (%)
PPPGMRPP	small nuclear ribonucleoprotein polypeptide B	ANX11	8–15	PPPGGYPP	75
			101–108	PPYGMYPP	
			107–114	PPPGGNPP	
			134–141	PPPGQQPP	
		CBP	873–880	TPPGMTPP	75
		VASP	172–179	PPPGPPPP	75
			178–185	PPPGPPPP	
PPPGMIPP	small nuclear ribonucleoprotein polypeptide A	ANX11	8–15	PPPGGYPP	75
			101–108	PPYGMYPP	
			107–114	PPPGGNPP	
			134–141	PPPGQQPP	
		CBP	873–880	TPPGMTPP	75
		VASP	172–179	PPPGPPPP	75
			178–185	PPPGPPPP	
GMIPPPGL	U1 small nuclear ribonucleoprotein A	ANX11	104–111	GMYPPPGG	75
		CBP	2114–2121	GMQPQPGL	75
		VASP	181–188	GPPPPPGL	75
PGMIPPPG	U1 small nuclear ribonucleoprotein A	ANX11	4–11	PGYPPPPG	75
			103–110	YGMYPPPG	
		CBP	2113–2120	PGMQPQPG	75
			2125–2132	PGMQPQPG	
		VASP	174–181	PGPPPPPG	75
			180–187	PGPPPPPG	
PPGMIPPP	U1 small nuclear ribonucleoprotein A	ANX11	102–109	PYGMYPPP	75
		CBP	874–881	PPGMTPPQ	75
		VASP	173–180	PPGPPPPP	75
			179–186	PPGPPPPP	
PAPGMRPP	U1 small nuclear ribonucleoprotein C	SYNJ1	1120–1127	PAPPQRPP	75
		CBP	686–693	PAPGAQPP	75
PPPPSLPG	unnamed protein product	ANX11	29–36	PPPPSMPP	75
		VASP	119–126	PPPPALPT	75
			183–190	PPPPGLPP	
PPGAMPPQ	U1 small nuclear ribonucleoprotein A	ANX11	140–147	PPGAYPGQ	75
		CBP	874–881	PPGMTPPQ	75

with an antigen index >1.5 between positions 171–184, which also corresponded well to several SLE epitopes based on the homologous alignment (Fig. 4B and Table 4). ANX11 and CBP also showed aligned fragments at several positions. However, protean software indicated that the antigenicity of CBP was generally <1, so it was not selected as a candidate antigen for further verification. The antigenicity of the 134–144 segments of ANX11 was higher but still not optimal, with a mean value below 1.5 (see Fig. 4C and D; Table S1, and Table S2).

Overall, we identified an optimal antigenic sequence of VASP that may induce autoreactivity and lead to the formation of autoantibodies in SLE.

3.5. Autoantibodies against VASP as a potential biomarker for demyelination in NPSLE

VASP contains an optimal antigenic sequence between 171 and 184. This peptide may induce autoreactivity via epitope spreading

Table 4
The sequence features of $VASP_{171\text{-}184}$ predicted by PROTEAN software.

Residue	Position	Turn	Coil	Hydrophilicity	Flexible	Antigenic Index	Surface Probability Plot
Pro	171	.	C	0.82	F	1.56	2.01
Pro	172	.	C	1.2	F	1.84	2.01
Pro	173	T	C	1.33	F	2.32	2.01
Pro	174	T	.	1.47	F	2.8	2.01
Gly	175	T	C	1.47	F	2.32	2.01
Pro	176	T	C	1.47	F	2.32	2.01
Pro	177	.	C	1.33	F	2.12	2.01
Pro	178	.	C	1.33	F	2.12	2.01
Pro	179	T	C	1.33	F	2.32	2.01
Pro	180	T	.	1.47	F	2.8	2.01
Gly	181	T	C	1.47	F	2.32	2.01
Pro	182	T	C	1.47	F	2.04	2.01
Pro	183	.	C	1.33	F	1.56	2.01
Pro	184	.	C	0.73	F	1.28	2.01

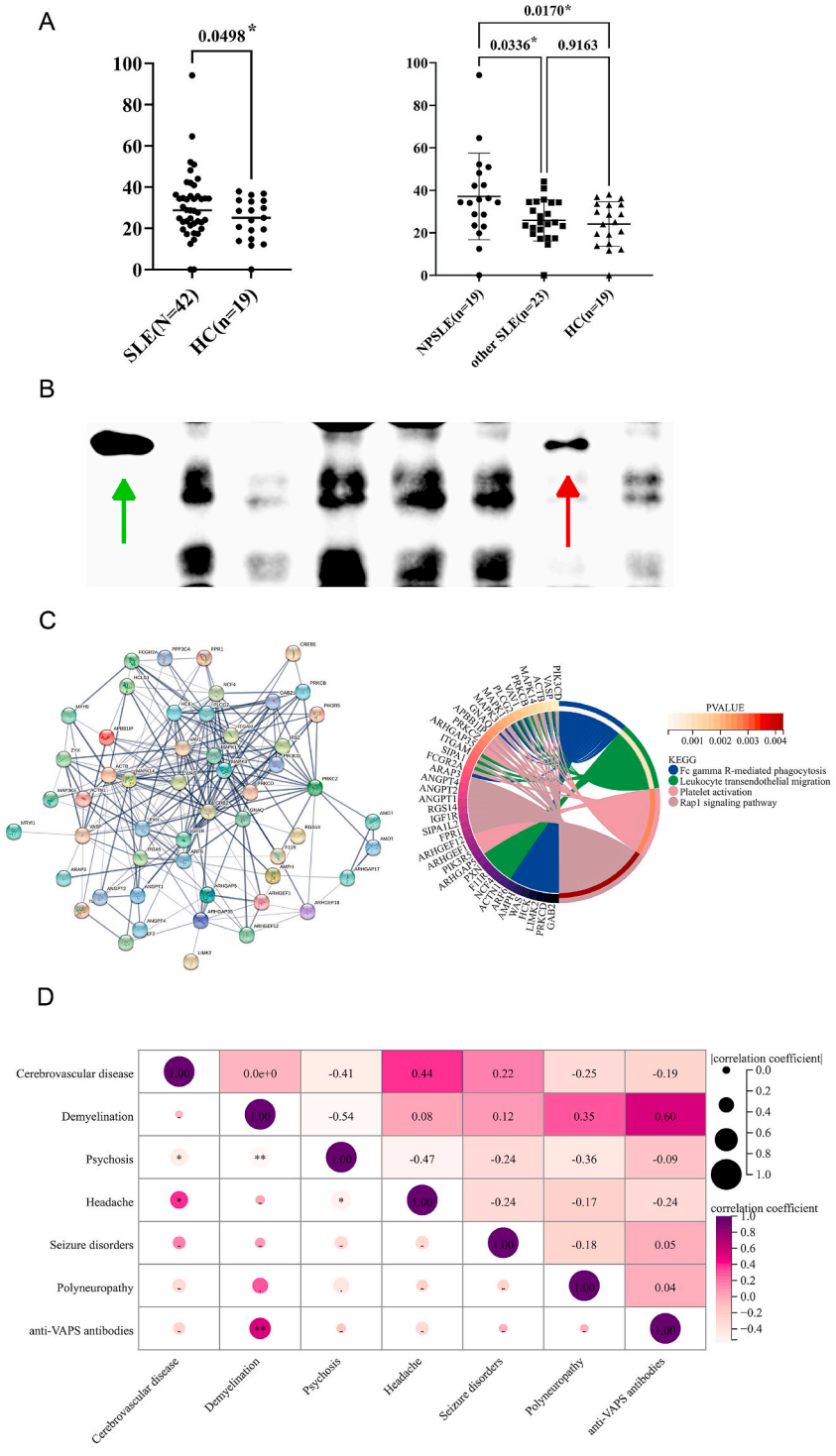

Fig. 5. (A) ELISA of anti-VASP autoantibodies with samples classified as SLE/HC or NPSLE/other SLE/HC. The vertical axis represents the normalized OD values. **(B)** Western blot showing the expression of anti-VASP autoantibodies. The green arrow indicates the position of positive control (complex of VASP and primary Ab), and the red arrow indicates the immunocomplex of VASP and its autoantibody from serum. **(C)** Protein-protein interaction network and functional enrichment of VASP and its adjacent proteins in blue/saddle brown modules. **(D)** The Correlation Matrix between anti-VASP Antibodies and psychoneurological symptoms.

with certain ribonucleoproteins, which share repetitive amino acid motifs [24,25]. To test this hypothesis, we randomly selected 42 SLE participants for further serum antibody detection, including 19 NPSLE and 23 patients without neuropsychiatric symptoms (other SLE group), and 19 HCs recruited from the physical examination center. Using ELISA, we observed higher levels of anti-VASP antibodies in SLE than in HCs. Further comparison of the OD values between NPSLE, other SLE, and HCs groups showed that patients with NPSLE had the highest levels of anti-VASP antibodies, followed by other SLE and HCs groups with no significant difference (Fig. 5A). A receiver operating characteristic (ROC) curve analysis suggested an optimal cutoff for diagnosing NPSLE and other SLE of 35.62, balancing sensitivity (0.47) and specificity (0.91) (Fig. S1F). We also performed ELISA for ANXA11, which, according to protean predictions, exhibited less optimal antigenicity. The antibody levels for ANXA11 showed no significant differences among the three groups (Fig. S1G).

Given the epitope similarity between VASP and U1-snRNP, we further tested antibodies against U1-snRNP and Sm to determine if the serum reactivity to VASP result from cross-reactivity. Correlation analysis between anti-U1-snRNP, anti-Sm, and anti-VASP antibodies revealed only a non-significant positive correlation. Furthermore, the positivity rates of anti-RNP and anti-SM in anti-VASP$^+$ NPSLE were both 62.5 %, while the positivity rates of anti-VASP in anti-RNP$^+$ and anti-SM$^+$ NPSLE were 38.5 % and 62.5 %, respectively. These findings suggested a certain overlap among the positive sera, indicating that VASP may serve as an independent marker with a complementary role in identifying NPSLE cases that are negative for anti-RNP and anti-SM (Figs. S1H–J).

Based on positive results by ELISA, we conducted immunoprecipitation experiments to validate the findings by capturing autoantibodies against VASP. Seven NPSLE serum samples with the highest OD values were subjected to Western blot analysis. The immunocomplexes were separated by gel electrophoresis and transferred to a membrane for detection. The presence of autoantibodies against VASP in one sample was observed, indicating immunocomplex formation between VASP and its autoantibodies (Fig. 5B).

VASP are actin-associated proteins involved in various processes dependent on cytoskeleton remodeling and cell polarity, such as axon guidance, lamellipodial and filopodial dynamics, platelet aggregation, and cell migration [26]. According to PPI networks, VASP and its adjacent proteins participate in platelet aggregation and Fc gamma R-mediated phagocytosis, which was consistent with the preceding results showing a relatively higher level of PLT in NPSLE (Fig. 5C).

Next, we examined links between specific neuropsychiatric symptom(s) and the novel antibodies, considering the clinical heterogeneity of NPSLE. Association analysis revealed correlations between several symptoms, such as cerebrovascular disease, headache, and seizure disorder, as well as between demyelination and polyneuropathy (Fig. 5D). When connecting them to anti-VASP antibodies, we found a strong positive correlation between antibodies and demyelination ($R = 0.60$, $p < 0.01$).

4. Discussion

SLE affects many organs, and 37–95 % of patients tend to experience neuropsychiatric manifestations [27]. Due to the polymorphic phenotype in NPSLE, numerous studies have tried to improve the diagnosis and explore the pathogenic mechanism, considering that identifying reliable biomarkers could be crucial in the management. Tsuchiya et al. (2014) employed a random peptide display library screening technique to identify GABARB subunits as potential antigens [28]. Lefranc et al. (2007) and Kimura et al. (2008) utilized SDS-PAGE and mass spectrometry, respectively, to investigate serum self-IgG reactivity against brain tissue and identified specific antigens, such as heat-shock protein, as targets of anti-endothelial cell antibodies [29,30]. Mader et al. (2018) used ELISA to confirm the significance of antibodies to DWEYS in demyelinating NPSLE [31]. These studies have identified promising biomarkers for NPSLE, and subsequent research has aimed to elucidate the pathogenic mechanisms underlying these antibodies. For instance, anti-NMDAR antibodies have been shown to cause selective impairment in spatial cognition [32]. Also, anti-ribosomal P protein antibodies may lead to cognitive impairment [33]. These important findings suggest that antibodies targeting pathogenic antigens in the neuron-related constituents might have a causal part in the development of NPSLE.

In various autoimmune antibody-mediated neurological syndromes, such as autoimmune encephalitis and demyelinating syndromes, the concentration of autoantibodies in the blood is higher than that in the cerebrospinal fluid, suggesting that in most cases, the autoantibodies are initially produced peripherally [34]. In this study, we employed homologous alignment to identify potential antigens in proteins corresponding to NPSLE-related genes. Our investigation led us to identify VASP as a potential autoantigen in NPSLE based on its sequence homology with snRNP. We confirmed the diagnostic value of VASP using ELISA with patient serum samples. Our study focused on epitope spreading, a phenomenon involving the interaction of T/B cells. Epitope spreading has been reported to occur within the U1-snRNP complex, with sequence homology being a potential driver [35]. Anti-ANA or anti-ENA antibodies often target snRNP and are frequently found at high levels in patients with NPSLE [25]. RNA binding motifs are commonly found in many RNA-containing antigens, and high sequence homology is observed in different subsets of RNP [36]. Furthermore, our analysis revealed no significant correlation between the levels of anti-U1-RNP/SM and VASP antibodies, thereby suggesting that VASP autoantibodies can serve as an independent marker for NPSLE. Our research demonstrated that omics-based results, even from transcriptome analysis, can be applied to autoantigen discovery in addition to traditional pathway analysis and function verification. These findings have important implications for the study of autoimmunity diseases.

Mader et al. (2018) used ELISA to directly compare the OD values between patients and control groups to represent antibody levels [31]. To ensure higher specificity in the validation experiment, we employed the adjusted OD value obtained by subtracting the no-protein-coated wells' absorbance from the protein-coated wells' absorbance. Considering the dysregulated autoantibody production observed in SLE, the background value, which indicates the rate of nonspecific antibody binding, was higher than in HC. Therefore, our design of comparing the adjusted OD values between groups rather than the absorbance of the protein-coated wells provided a more reliable and accurate evaluation of the results.

As previously stated, VASP is highly expressed in platelet and brain tissue and is important in platelet activation and FcγR-mediated

immunology (Fig. 5C). Besides, our phenotypic association and WGCNA analysis revealed that hub genes and NPSLE involvement are positively related to the platelet level (Figs. 1A and 2D). Moreover, given that the most common symptoms observed are cerebrovascular disease and demyelination (Table 2), the nerve injury in our NPSLE population may be due to dysregulated coagulation to a great extent. A recent study has demonstrated that activated platelets can release antigenic nuclear components through FcγR [8], implying that the antibodies against VASP may originate from epitope spreading of platelet-released nuclear antigens due to abnormal platelet activation.

The present study has several limitations. First, compared to previous studies using antibody microarrays, which comprehensively assess potential antigens [28–30], our approach utilized existing epitope data and employed an epitope comparison method for preliminary screening. While this method is more cost-effective and time-efficient, it may not be as exhaustive, potentially overlooking other relevant antigens. Second, although we identified antibodies against VASP, further exploring its mechanisms of action, such as whether they cause cognitive impairments similar to anti-NMDAR and anti-ribosomal P protein antibodies, is required [32,33], which we plan to do in future studies. Third, our study's relatively small sample size may limit our findings' generalizability. Further research is needed to validate the potential of this novel biomarker for distinguishing NPSLE from other neurological autoimmune diseases. Additionally, future studies should aim to elucidate the underlying biological mechanisms associated with anti-VASP antibodies.

Overall, given the great challenge for clinicians to select appropriate treatment modalities for NPSLE based on empirical judgment alone, our identification of anti-VASP antibody as a potential biomarker could optimize the diagnosis and clinical guidance. Moreover, our findings suggest the involvement of VASP and its antibodies in NPSLE and their linkage with platelets, which could serve as a foundation for further investigations in this field. Such studies could further elucidate the pathogenic mechanisms underlying this complex disease.

Data availability statement

The raw sequence data reported in this paper have been deposited in the Genome Sequence Archive (Genomics, Proteomics & Bioinformatics 2021) in National Genomics Data Center (Nucleic Acids Res 2022), China National Center for Bioinformation/Beijing Institute of Genomics, Chinese Academy of Sciences (GSA-Human: HRA008095) that are publicly accessible at https://ngdc.cncb.ac.cn/gsa-human.

Funding statement

The study was supported by the National Natural Science Foundation of China (No.82001728) and the Department of Science and Technology of Sichuan Province (No.2019YJ013 and No.2022YFH0023).

Ethics approval statement

This work has been carried out in accordance with the Declaration of Helsinki (2000) of the World Medical Association. This work was approved by the Clinical Trial Ethics Committee, West China Hospital of Sichuan University (HX-IRB-AF-14-V3.0).

Patient consent statement

All participants provided informed consent.

Permission to reproduce material from other sources

Not applicable.

Clinical trial registration

Not applicable.

CRediT authorship contribution statement

Chenxi Zhu: Writing – original draft, Data curation, Conceptualization. **Yan Liu:** Methodology, Writing – original draft. **Jiayi Xu:** Methodology, Formal analysis. **Hang Yang:** Investigation, Formal analysis. **Yi Zhao:** Writing – review & editing, Data curation. **Yi Liu:** Formal analysis, Data curation, Formal analysis, Data curation.

Declaration of competing interest

The authors declare that they have no known competing financial interests or personal relationships that could have appeared to influence the work reported in this paper.

Acknowledgments

None.

List of abbreviations

NPSLE	Neuropsychiatric systemic lupus erythematosus
ELISA	enzyme-linked immunosorbent assay
VASP	vasodilator-stimulated phosphoprotein
SLE	Systemic lupus erythematosus
WGCNA	weighted gene co-expression network analysis
TOM	topological overlap matrix
PPI	Protein-Protein Interaction
HRP	horseradish peroxidase
ESR	erythrocyte sedimentation rate
BUN	blood urea nitrogen

Appendix A. Supplementary data

Supplementary data to this article can be found online at https://doi.org/10.1016/j.heliyon.2024.e37110.

References

[1] A. Kaul, et al., Systemic lupus erythematosus, Nat. Rev. Dis. Prim. 2 (1) (2016) 16039.
[2] G. Flores-Mendoza, et al., Mechanisms of tissue injury in lupus nephritis, Trends Mol. Med. 24 (4) (2018) 364–378.
[3] S. Caielli, Z. Wan, V. Pascual, Systemic lupus erythematosus pathogenesis: interferon and beyond, Annu. Rev. Immunol. (2023) 533–560.
[4] D. Mevorach, et al., Systemic exposure to irradiated apoptotic cells induces autoantibody production, J. Exp. Med. 188 (2) (1998) 387–392.
[5] G.C. Tsokos, et al., New insights into the immunopathogenesis of systemic lupus erythematosus, Nat. Rev. Rheumatol. 12 (12) (2016) 716–730.
[6] S.E. Degn, et al., Clonal evolution of autoreactive germinal centers, Cell 170 (5) (2017) 913–926.e19.
[7] H.R. Thiam, et al., Cellular mechanisms of NETosis, Annu. Rev. Cell Dev. Biol. 36 (2020) 191–218.
[8] I. Melki, et al., Platelets release mitochondrial antigens in systemic lupus erythematosus, Sci. Transl. Med. 13 (581) (2021).
[9] H. Lou, G.S. Ling, X. Cao, Autoantibodies in systemic lupus erythematosus: from immunopathology to therapeutic target, J. Autoimmun. 132 (2022) 102861.
[10] A. Fanouriakis, et al., Update on the diagnosis and management of systemic lupus erythematosus, Ann. Rheum. Dis. 80 (1) (2021) 14–25.
[11] J.M. Guthridge, C.A. Wagner, J.A. James, The promise of precision medicine in rheumatology, Nat. Med. 28 (7) (2022) 1363–1371.
[12] M. Aringer, et al., 2019 European league against rheumatism/American College of rheumatology classification criteria for systemic lupus erythematosus, Arthritis Rheumatol. 71 (9) (2019) 1400–1412.
[13] The American College of Rheumatology nomenclature and case definitions for neuropsychiatric lupus syndromes, Arthritis Rheum. 42 (4) (1999) 599–608.
[14] B. Zhang, S. Horvath, A general framework for weighted gene co-expression network analysis, Stat. Appl. Genet. Mol. Biol. 4 (2005) Article17.
[15] M.I. Love, W. Huber, S. Anders, Moderated estimation of fold change and dispersion for RNA-seq data with DESeq2, Genome Biol. 15 (12) (2014) 550.
[16] T. Wu, et al., clusterProfiler 4.0: a universal enrichment tool for interpreting omics data, Innovation 2 (3) (2021) 100141.
[17] D Szklarczyk, et al., The STRING database in 2023: protein-protein association networks and functional enrichment analyses for any sequenced genome of interest, Nucleic Acids Res. 51 (1) (2023) 638–646.
[18] H.H. Bui, et al., Development of an epitope conservancy analysis tool to facilitate the design of epitope-based diagnostics and vaccines, BMC Bioinf. 8 (2007) 361.
[19] X. Wang, et al., Synaptic dysfunction in complex psychiatric disorders: from genetics to mechanisms, Genome Med. 10 (1) (2018) 9.
[20] S.E. Henrickson, et al., T cell sensing of antigen dose governs interactive behavior with dendritic cells and sets a threshold for T cell activation, Nat. Immunol. 9 (3) (2008) 282–291.
[21] D. Baumjohann, et al., Persistent antigen and germinal center B cells sustain T follicular helper cell responses and phenotype, Immunity 38 (3) (2013) 596–605.
[22] R. Vita, et al., The immune epitope database (IEDB): 2018 update, Nucleic Acids Res. 47 (D1) (2019) D339–d343.
[23] UniProt: the universal protein knowledgebase in 2021, Nucleic Acids Res. 49 (D1) (2021) D480–d489.
[24] Z. Zhao, et al., Nature of T cell epitopes in lupus antigens and HLA-DR determines autoantibody initiation and diversification, Ann. Rheum. Dis. 78 (3) (2019) 380–390.
[25] N.H. Kattah, M.G. Kattah, P.J. Utz, The U1-snRNP complex: structural properties relating to autoimmune pathogenesis in rheumatic diseases, Immunol. Rev. 233 (1) (2010) 126–145.
[26] S. Li Calzi, et al., Carbon monoxide and nitric oxide mediate cytoskeletal reorganization in microvascular cells via vasodilator-stimulated phosphoprotein phosphorylation: evidence for blunted responsiveness in diabetes, Diabetes 57 (9) (2008) 2488–2494.
[27] I. Carrión-Barberà, et al., Neuropsychiatric involvement in systemic lupus erythematosus: a review, Autoimmun. Rev. 20 (4) (2021) 102780.
[28] H. Tsuchiya, et al., Identification of novel autoantibodies to GABA(B) receptors in patients with neuropsychiatric systemic lupus erythematosus, Rheumatology 53 (7) (2014) 1219–1228.
[29] D. Lefranc, et al., Characterization of discriminant human brain antigenic targets in neuropsychiatric systemic lupus erythematosus using an immunoproteomic approach, Arthritis Rheum. 56 (10) (2007) 3420–3432.
[30] A. Kimura, et al., Proteomic analysis of autoantibodies in neuropsychiatric systemic lupus erythematosus patient with white matter hyperintensities on brain MRI, Lupus 17 (1) (2008) 16–20.
[31] S. Mader, et al., Understanding the antibody repertoire in neuropsychiatric systemic lupus erythematosus and neuromyelitis optica spectrum disorder: do they share common targets? Arthritis Rheumatol. 70 (2) (2018) 277–286.
[32] E.H. Chang, et al., Selective impairment of spatial cognition caused by autoantibodies to the N-Methyl-D-Aspartate receptor, EBioMedicine 2 (7) (2015) 755–764.
[33] M. Bravo-Zehnder, et al., Anti-ribosomal P protein autoantibodies from patients with neuropsychiatric lupus impair memory in mice, Arthritis Rheumatol. 67 (1) (2015) 204–214.

[34] S. Ramanathan, et al., Origins and immunopathogenesis of autoimmune central nervous system disorders, Nat. Rev. Neurol. 19 (3) (2023) 172–190.
[35] S. Barakat, et al., Mapping of epitopes on U1 snRNP polypeptide A with synthetic peptides and autoimmune sera, Clin. Exp. Immunol. 86 (1) (1991) 71–78.
[36] S. Hirohata, et al., Role of serum autoantibodies in blood brain barrier damages in neuropsychiatric systemic lupus erythematosus, Clin. Exp. Rheumatol. 36 (6) (2018) 1003–1007.